The redox-sensitive cation channel TRPM2 modulates phagocyte ROS production and inflammation

Anke Di[1], **Xiao-Pei Gao**[1], **Feng Qian**, **Takeshi Kawamura**, **Jin Han**, **Claudie Hecquet**, **Richard D. Ye**, **Stephen M. Vogel**, and **Asrar B. Malik**[*]

Department of Pharmacology and Center for Lung and Vascular Biology, College of Medicine, University of Illinois, Chicago, IL, 60612

Abstract

The NADPH oxidase activity of phagocytes and its generation of reactive oxygen species (ROS) is critical for host-defense, but ROS overproduction can also lead to inflammation and tissue injury. Here we report that TRPM2, a non-selective and redox-sensitive cation channel, inhibits ROS production in phagocytic cells and prevents endotoxin-induced lung inflammation in mice. TRPM2-deficient mice challenged with endotoxin (lipopolysaccharide) showed an increased inflammatory signature and decreased survival compared to controls. TRPM2 functions by dampening NADPH oxidase-mediated ROS production through depolarization of the plasma membrane in phagocytes. Since ROS also activates TRPM2, our findings establish a negative feedback mechanism inactivating ROS production through inhibition of the membrane potential-sensitive NADPH oxidase.

NADPH oxidase-dependent reactive oxygen species (ROS) production in phagocytic cells in response to infection plays a key role in the mechanism of inflammation [1, 2]. Multiple mechanisms including plasma membrane potential changes [3, 4], calcium (Ca^{2+}) influx, and Ca^{2+}-dependent protein kinase Cα (PKCα) activation [5, 6] induce NADPH oxidase activation. PKCα phosphorylates the Nox2 subunit p47^{phox} resulting in its translocation to the plasma membrane, which is needed for the assembly of the oxidase complex [6]. Transient receptor potential-melastatin 2 (TRPM2, also called LTRPC-2 or TRPC7 [7, 8]) is a non-selective cation channel permeable to Na^+ and Ca^{2+} (selectivity of TRPM2 for Ca^{2+} over Na^+ is 0.5-1.6 [9]). To date, most studies have addressed the influx of Ca^{2+} through the redox-sensitive TRPM2 channel[8, 10, 11]. We surmised that TRPM2-induced Ca^{2+} influx should enhance NADPH oxidase activation through activation of Ca^{2+} dependent PKC isoforms [5, 6]; however, our studies reported herein show that TRPM2 activation reduces NADPH oxidase-activated ROS production while at the same time increasing membrane depolarization . We addressed the mechanism of TRPM2 regulation of ROS production in

[*]*Corresponding author:* Department of Pharmacology, The University of Illinois, College of Medicine 835 South Wolcott Avenue, Chicago, IL, 60612 Phone: (312) 996-7635; Fax: (312) 996-1225; abmalik@uic.edu.
[1]These authors contributed equally to this work.

phagocytes and its relationship to membrane potential changes and the functional significance of TRPM2 in mediating endotoxin (lipopolysaccharides, LPS) - induced lung inflammatory injury. We show using a patch clamping approach combined with biochemistry a strong correlation between reduced ROS production and plasma membrane depolarization caused by TRPM2 activation in phagocytic cells. TRPM2 activation increased survival of endotoxemic mice and decreased lung oxidative damage as well as production of inflammatory cytokines and chemokines. Thus, TRPM2, a non-selective cation channel, protects the lung from inflammatory injury by dampening NADPH oxidase activity in phagocytes and lowering ROS production.

RESULTS

Protective role of TRPM2 in lung inflammation

In the dextran sulfate sodium (DSS)-induced model of colitis, chemokine production, polymorphonuclear leukocyte (PMN) infiltration, and ulceration were reduced in TRPM2 knockout mice ($Trpm2^{-/-}$)[12]. We therefore examined whether $Trpm2^{-/-}$ mice were similarly protected in an endotoxin-induced lung inflammation model. Contrary to DSS-induced colitis inflammation, we observed augmented release of chemokines and proinflammatory cytokines, tumor necrosis factor (TNF), macrophage inflammatory protein 2 (MIP-2), and interleukin 6 (IL-6) in $Trpm2^{-/-}$ mouse lungs compared to $Trpm2^{+/+}$ mice (Fig. 1a-c). LPS also induced significantly greater lung tissue myeloperoxidase (MPO) activity in $Trpm2^{-/-}$ than $Trpm2^{+/+}$ mice (Fig. 1d) indicating augmented sequestration of inflammatory PMN in knock-out mouse lungs. Inflammation induced by LPS is characterized by rapid PMN sequestration in response to release of chemokines and cytokines after activation of the redox-sensitive pro-inflammatory transcription factor NF-κB [13]. Increased expression of NF-κB was also seen in the lungs of $Trpm2^{-/-}$ mice during LPS-induced inflammation (Supplementary Fig. 1). Furthermore, augmented lung inflammatory cell infiltration, greater lung edema, and decreased survival were observed in the LPS challenged $Trpm2^{-/-}$ mice (Figure 1e-g). These results demonstrate a protective role of TRPM2 in LPS-induced lung inflammation.

Oxidative lung injury in TRPM2 deficient mice

Since ROS is crucial for the mechanism of lung inflammation and injury[14], we next determined whether TRPM2 participates in regulating ROS production. Given that TRPM2 is a non-selective cation channel permeable to Na^+ and Ca^{2+}, we initially hypothesized that it mediates ROS production in phagocytes by conducting Ca^{2+} into cells [6]. However, $Trpm2^{-/-}$ mice had augmented ROS production from PMN and bone marrow derived macrophages (BMDM) stimulated with LPS or phorbol-12 myristate-13 acetate (PMA) (Figure 2a-d). The increased ROS production required NADPH oxidase since diphenyleneiodonium (DPI, an inhibitor of NADPH oxidase[15]) prevented ROS production in both $Trpm2^{+/+}$ and $Trpm2^{-/-}$ macrophages (Figure 2c). To confirm an inhibitory role of TRPM2 in ROS production, we used DPQ {(3,4-dihydro-5-[4-(1-piperidinyl)butoxyl]-1(2H)-isoquinolinone}, a cell-permeable poly-ADP-ribose polymerase inhibitor (PARP), which prevents adenosine diphosphoribose (ADPR) generation, to block TRPM2 channel function [16, 17]. ROS production from $Trpm2^{+/+}$ macrophages pretreated

with DPQ (100 μM for 30 minutes) was increased to the level seen in *Trpm2⁻/⁻*
macrophages, whereas DPQ pretreatment did not further increase ROS release from
Trpm2⁻/⁻ macrophages (Figure 2c,d). To elaborate further on TRPM2's role in blocking
ROS production, we determined intracellular ROS levels in *Trpm2⁺/⁺* and *Trpm2⁻/⁻*
macrophages. ROS production in cells from *Trpm2⁻/⁻* mice challenged with PMA or live
Escherichia coli was significantly increased compared to *Trpm2⁺/⁺* mice cells
(Supplementary Figure 2a). *Trpm2⁻/⁻* mice also showed less bacterial burden compared to
wild type (Supplementary Figure 2b), whereas the extent of phagocytosis was unaltered
(Supplementary Figure 2c). To evaluate the contribution of oxidative damage in mediating
lung inflammatory injury seen in *Trpm2⁻/⁻* mice, we first used immunochemistry to assess
8-hydroxydeoxyguanosine (8OHdG) levels (a sensitive marker of oxidative damage of
DNA [18, 19]) in mouse lungs. 8OHdG expression in *Trpm2⁻/⁻* lungs was markedly greater
than in *Trpm2⁺/⁺* lungs (Figure 2e, f). The increased TNF production by macrophages from
Trpm2⁻/⁻ mice was reduced to the same level seen in macrophages from *Trpm2⁺/⁺* mice
when the former cells were treated with DPI (Figure 2g). We also observed augmented
injury of endothelial cells interacting with LPS-stimulated macrophages from *Trpm2⁻/⁻*
mice compared to macrophages from *Trpm2⁺/⁺* mice (Supplementary Figure 3), indicating
greater potential of TRPM2 null phagocytes to injure the interacting target cells (in this case
endothelial cells) than wild type phagocytes. These results show that inhibition of
phagocytic cell ROS production is an important mechanism of TRPM2-mediated protection
in LPS-induced inflammation.

TRPM2 modulation of membrane potential regulates ROS

We next investigated the mechanism of TRPM2 inhibition of ROS production in phagocytic
cells. We initially surmised that TRPM2 as a Ca^{2+} permeable channel would induce ROS
production because of the role of Ca^{2+} in activating NADPH oxidase through Ca^{2+}-
dependent PKCα in phagocytes [6]; however, the marked ROS production persistent in the
absence of TRPM2 activation (Figure 2a-d) pointed to another pathway. Indeed PMA-
induced activation of PKCα in BMDM was unchanged regardless of TRPM2 expression
(Figure 3a). Moreover, p47*phox* phosphorylation induced by PMA was similar between
Trpm2⁻/⁻ and *Trpm2⁺/⁺* macrophages (Figure 3b), suggesting that the mechanism of ROS
production in *Trpm2⁻/⁻* macrophages lies beyond NADPH oxidase complex assembly. Thus,
we tested the hypothesis that TRPM2 controls ROS production through regulating the
membrane potential of phagocytes because NADPH oxidase activity and membrane
potential are linked [3, 4, 20]. We measured ROS production at different membrane potentials
induced by changing the extracellular potassium (K^+) concentration. A strong correlation
was seen between decreased membrane potential (depolarization) and increased extracellular
K^+ in mouse BMDM (Supplementary Figure 4). Likewise increased ROS production in
Trpm2⁻/⁻ macrophages was reduced to the level seen in *Trpm2⁺/⁺* macrophages when
membrane potential was controlled at the same level by increasing extracellular K^+ (to 120
mM) in both *Trpm2⁻/⁻* and *Trpm2⁺/⁺* macrophages (Figure 3c, d). We next determined using
patch clamping whether TRPM2 activation directly altered the membrane potential. ADPR ,
a potent activator of TRPM2 [8], added through a patching pipette significantly depolarized
the plasma membrane (from −78 ± 6 mV to −14 ± 6 mV) in *Trpm2⁺/⁺* macrophages but not
in the *Trpm2⁻/⁻* macrophages (from −82 ± 5 mV to −74 ± 7 mV) (Figure 4a, b). Although

PMA depolarized the plasma membrane of both $Trpm2^{+/+}$ macrophages (from -81 ± 2 mV to -10 ± 4 mV) and $Trpm2^{-/-}$ macrophages (from -82 ± 2 mV to -50 ± 8), it caused a significantly lower depolarization in $Trpm2^{-/-}$ macrophages (Figure 4c, d). This difference in membrane potential between $Trpm2^{+/+}$ and $Trpm2^{-/-}$ cells and its relationship to ROS release is shown in Figure 4e.

To validate the hypothesis that TRPM2 regulates ROS production through altering the membrane potential, we next addressed the role of Na^+ entry through TRPM2 in mediating inhibition of ROS production. First we determined whether ROS production can be restored to normal levels in $Trpm2^{-/-}$ macrophages by providing an artificial cationic conductance with gramicidin, a non-selective Na^+ -permeable channel that depolarizes the plasma membrane [21, 22]. ROS production induced by PMA in both $Trpm2^{+/+}$ and $Trpm2^{-/-}$ macrophages was reduced to the same level in the presence of gramicidin (40μg/ml) (Figure 4f). We also determined the contribution of Na^+ entry through TRPM2 in regulating ROS production by measuring changes in ROS production elicited by PMA in solution containing N-methyl-D-glucamine (NMDG) instead of Na^+. We surmised that Na^+ removal should mimic the effects of TRPM2 ablation and $Trpm2^{+/+}$ cells should therefore produce more ROS in the presence of NMDG. Substitution of Na^+ by NMDG augmented ROS production in $Trpm2^{+/+}$ cells whereas it had little effect in $Trpm2^{-/-}$ cells (Figure 4f). These results together demonstrate that TRPM2 profoundly downregulates NADPH oxidase-mediated ROS production through cation influx-dependent depolarization of plasma membrane potential (see illustration in Supplemental Figure 5) .

LPS activates TRPM2 through ROS generation

TRPM2 can be activated by binding of ADPR to the nudix-box (NUDT9-H) in its C terminus [23-25] and through ROS-mediated generation of ADPR [26]. Addition of 200 μM ADPR through the patch pipette elicited a linear, non-selective cation current in both PMN and BMDM and isosmotic replacement of external Na^+ by the impermeant organic cation NMDG abolished the inward current (Supplemental Figure 6a-d). $Trpm2^{-/-}$ PMN and $Trpm2^{-/-}$ BMDM failed to respond to ADPR. We also determined TRPM2 activation by H_2O_2, a known TRPM2 activating ROS [27, 28]. Perfusion of cells with H_2O_2 (300 μM) elicited a non-selective cation current in $Trpm2^{+/+}$ PMN and isosmotic replacement of external Na^+ by NMDG abolished the inward current**.** Although perfusion of cells with H_2O_2 also activated a small outward current in $Trpm2^{-/-}$ cells, H_2O_2 failed to induce this current in $Trpm2^{-/-}$ cells (Supplemental Figure 6e). Blocking the inward Na^+ current with NMDG resulted in left-shift in the reversal potential (membrane potential at zero transmembrane current; inset in Supplemental Figure 6e shows the shift). These findings demonstrate that the cells are hyperpolarized in the absence of Na^+, therefore favoring ROS production.

We took advantage of TRPM2 permeability to Ca^{2+} to study TRPM2 activation by monitoring Ca^{2+} influx using fura-2. LPS (1μg/ml) added to extracellular medium induced a transient increase of intracellular Ca^{2+} in BMDM from $Trpm2^{+/+}$ mice (Figure 5a, b). The intracellular Ca^{2+} ($[Ca^{2+}]_i$) increase induced by LPS was significantly reduced in cells from $Trpm2^{-/-}$ mice. The LPS-induced $[Ca^{2+}]_i$ increase was also sensitive to NADPH oxidase

inhibition using DPI (Figure 5a,b). These results show that LPS-induced production of ROS activates TRPM2.

We also used fura-2 to measure $[Ca^{2+}]_i$ increase induced by H_2O_2. $[Ca^{2+}]_i$ increase induced by H_2O_2 was significantly reduced in the cells from $Trpm2^{-/-}$ mice (Figure 5c,d). The increase in $[Ca^{2+}]_i$ in $Trpm2^{+/+}$ macrophages pretreated with DPQ (100 μM) was reduced to the level seen in $Trpm2^{-/-}$ macrophages, whereas DPQ produced no further decrease $[Ca^{2+}]_i$ in $Trpm2^{-/-}$ macrophages (Figure 5c,d). These results show the key role of ADPR in mediating ROS-induced activation of TRPM2.

Compensation for Ca^{2+} entry secondary to TRPM2 deletion

We next addressed the possibility that TRPM2 deletion may lead to enhanced Ca^{2+} signaling induced by stimuli through other redox-sensitive Ca^{2+} channels. We determined changes in intracellular Ca^{2+} induced by platelet-activating factor (PAF), a Ca^{2+}-mobilizing agonist [29] that fails to induce oxidative burst (except at very high concentration ~1μM)[30]. We therefore avoided any confounding effect of the ensuing membrane depolarization to reduce the driving force for Ca^{2+} entry in cells as shown above. Addition of PAF (0.1 μM) increased $[Ca^{2+}]_i$ with two-peaks, a initial rapid response with high amplitude followed by a slow, lower amplitude response in cells from both $Trpm2^{+/+}$ and $Trpm2^{-/-}$ mice (Figure 5e,f). Importantly, PAF did not induce ROS production in BMDM from both $Trpm2^{+/+}$ and $Trpm2^{-/-}$ mice (Supplemental Fig. 7). There was also no difference in $[Ca^{2+}]_i$ increase induced by PAF between $Trpm2^{+/+}$ and $Trpm2^{-/-}$ BMDM (Figure 5e,f). Therefore TRPM2 deletion did not increase $[Ca^{2+}]_i$ induced by PAF in the absence of ROS production.

Since compensatory ion channel expression and activation may be induced in the knockout mouse model, we next determined whether Ca^{2+}-activation of the non-selective cation (CAN) channels [31, 32] is altered in $Trpm2^{-/-}$ cells. CAN channels were studied since they also regulate membrane potential[33]. TRPM4 and TRPM5 have been identified as two CAN class channels [31, 32, 34, 35]. Addition of 100 μM Ca^{2+} through the patch pipette elicited a highly outward rectified non-selective cation current in both $Trpm2^{+/+}$ and $Trpm2^{-/-}$ macrophages (Supplemental Figure 8). The property of this outward rectified current (the amplitude of the current at positive potential is greater than the currents at negative potential) induced by Ca^{2+} is consistent with reports about TRPM4 and TRPM5[32, 34, 35]. Our results show that CAN (or TRPM4 and TRPM5) activation was not affected by TRPM2 deletion (Supplemental Figure 8). Thus, TRPM2 deletion was not compensated by changes in activation of other related family members, TRPM4 and TRPM5, and compensation of these channels is unlikely to explain the marked differences in lung inflammatory injury between $Trpm2^{+/+}$ and $Trpm2^{-/-}$ mice shown above.

DISCUSSION

TRPM2 has been found in many cell types of the immune system, including dendritic cells (DCs), PMN, monocytes, macrophages and lymphocytes [36, 37] however the function of TRPM2 in these cells has remained elusive. The oxidant-dependent mechanism of activation of TRPM2 suggests the involvement of this channel in pathogenic processes such as carcinogenesis, inflammation, ischemia-reperfusion injury, neurodegenerative disorders and

diabetes (see review [37]). In these studies, TRPM2 channel has emerged as an important Ca^{2+} signaling mechanism contributing to cellular functions such as cytokine production, insulin release, cell motility and cell death [37]. In DCs, TRPM2 regulates intracellular Ca^{2+} levels and is required for optimal DC maturation and chemotaxis [36]. DCs express TRPM2 preferentially in endolysosomal compartments, which release Ca^{2+} on exposure to intracellular ADPR or stimulation by chemokines. In monocytes, the impairment of chemokine production in cells lacking TRPM2 was linked to a defect in TRPM2-mediated Ca^{2+} influx [12, 37]. Our study reveals a novel TRPM2 function in which TRPM2 acts as an essential modulator of plasma membrane potential by conducting the influx of cations including both Ca^{2+} and Na^{+}. Our results in phagocytic cells show that activation of the redox-sensitive TRPM2 inhibits ROS production suggesting that TRPM2 serves as a crucial negative feedback mechanism of ROS production.

The question arises how TRPM2, a member of the TRP family of non-selective cation channels, down-regulates ROS production. Superoxide (O_2^{-}) is generated upon NADPH oxidase assembly and activation through transfer of electrons from cytosolic NADPH to extracellular oxygen [38, 39]. Electron flux associated with membrane depolarization [40] would therefore inhibit any further transfer of electrons across the membrane by NADPH oxidase if a compensating charge is not provided. This could explain the voltage dependence of NADPH oxidase activity [4, 41]. To facilitate ROS production, the transferred extracellular electrons must be neutralized by protons (H^{+}) transported extracellularly through voltage-gated proton channels [3, 42]. Voltage-gated proton channels are open when the plasma membrane is depolarized during NADPH oxidase activation. By moving positive charge (Ca^{2+} and Na^{+}) across the plasma membrane, TRPM2 induces membrane depolarization and thereby inhibits electrogenic activity of NADPH oxidase and blocks O_2^{-} production. Although there is no doubt about the voltage-dependent nature of NADPH oxidase activity, the range of voltage-dependence has varied in different studies. It was reported that NADPH oxidase is voltage-independent from −100 mV to >0 mV [3], but it is steeply inhibited by further depolarization, and abolished at about +190 mV [3]. It was later shown that NADPH oxidase activity is markedly voltage-dependent, which steeply decreases with depolarization within the physiological membrane potential range (−60 to 60 mV). The previously described apparent voltage-independence was attributed to limitation of the substrate, NADPH, and not to any intrinsic property of NADPH oxidase [41]. We show that TRPM2 is a non-selective cation channel which conducts positive charge (Ca^{2+} and Na^{+}) into phagocytes and thus suppresses NADPH oxidase activity when the plasma membrane is negative. Under these conditions, TRPM2 activation is expected to reduce electron transfer through NADPH oxidase by carrying cations into cells. These results thus identify the key role of TRPM2-dependent inhibition of NADPH oxidase activity in inactivating ROS production.

Ion channels play a critical role in the array of pathological responses to sepsis [43, 44]. The sepsis mediator LPS can either activate or inhibit ion channels [44, 45]. Our study describes a protective anti-inflammatory role for TRPM2 in LPS-induced lung injury and it demonstrates a previously unknown function of TRPM2 in dampening phagocytic cell NADPH oxidase-mediated ROS production. TRPM2 mediates transmembrane flux of cations down the electrochemical gradient, raising intracellular cation concentration and

depolarizing the plasma membrane. The depolarization inhibits ROS production in phagocytes and prevents lung inflammatory injury induced by LPS. These findings uncover an intrinsic negative feedback mechanism that functions at the level of the assembled NADPH oxidase complex. TRPM2 activation in phagocytic cells during sepsis may thus have a unique ability to prevent NADPH oxidase-derived ROS production and thereby protect the host against inflammation and tissue injury.

METHODS

Mice, cell cultures, and reagents

C57 black 6 (C57BL6) mice were obtained from Charles River Laboratory. *Trpm2*$^{-/-}$ C57BL/6 mice were a gift from Dr Barbara A Miller (Penn State, PA). *Trpm2*$^{-/-}$ mice were backcrossed with C57BL6 mice for 5 generations to eliminate any background effects on the observed phenotypes. *Trpm2*$^{-/-}$ and wild-type (*Trpm2*$^{+/+}$) littermates were used in the present studies. All mice were housed in the University of Illinois Animal Care Facility in accordance with institutional and NIH guidelines. Veterinary care of these animals and related animal experiments was approved by the University of Illinois Animal Resources Center (Chicago, IL). Mouse bone marrow derived macrophage (BMDM) were isolated and cultured as described [46]. Mouse PMN (polymorphonuclear leukocyte) were isolated from murine bone marrow using Percoll density gradients as described [47]. Mouse lung vascular endothelial cells (MLVECs) were isolated from *Trpm2*$^{+/+}$ and *Trpm2*$^{-/-}$ mice as described [48]. Phorbol-12-myristate-13-acetate (PMA), lipopolysaccharides (LPS, from *Escherichia coli* 0111:B4), hydrogen peroxide (H$_2$O$_2$) were purchased from Sigma. PKCα, p47, P-PKCα antibodies and antibody that recognizes p47^{phox} phosphorylation at Ser473 were purchased from Cell Signaling.

Whole cell recordings

Electrophysiological recordings were obtained using a voltage-clamp technique. All experiments were conducted at room temperature (22 - 24^0 C) using an EPC-10 patch clamp amplifier (HEKA Electronik GmbH, Lambrecht, Germany) and using the Pulse V 8.8 acquisition program (HEKA Electronik GmbH, Lambrecht, Germany). TRPM2 whole cell current were measured using method similar to those described earlier[8]. Currents were elicited by using a series of test pulses range from −110 to +110 mV (test pulses were 200 ms in duration and delivered at 2 s intervals). The holding potential was 0 mV. The pipette solution contained (in mM): 135 CsSO$_3$CH$_3$, 8 NaCl, 2 MgCl$_2$, 0.5 CaCl$_2$, 1EGTA and 10 Hepes, pH 7.2. ADPR (200 μM) or PMA (1μM) were included in the pipette solution or H$_2$O$_2$ (300 μM) was perfused to the cells in order to induce TRPM2 current. To induce Ca^{2+}-activated cation currents, 100 μM free [Ca^{2+}]$_i$ was included in the pipette solution. The bath solution contained (in mM): 145 NaCl, 2 CaCl$_2$, 1 MgC$_2$, 10 HEPES, pH 7.4. In some experiments, 145 NaCl in the bath solution was replaced by 145 N-methyl-D-glucamine (NMDG). In perforated patch clamp, about 500 mg solubilized amphotericin B was added in the pipette solution. Whole cell current was analyzed using IGOR software (WaveMetrics, Lake Oswego, OR).

Plasma membrane potential recordings

Plasma membrane potential was recorded by current clamp. The pipette solution contained (in mM): 135 KCl, 8 NaCl, 2 MgC$_2$, 0.5 CaC$_2$, 1EGTA and 10 Hepes, pH 7.2. The bath solution contained (in mM): 5 KCl, 140 NaCl, 2 CaCl$_2$, 1 MgC$_2$, 10 HEPES, pH 7.4. In order to study the effect of different extracellular potassium (K$^+$) concentration on membrane potential in resting cells, sodium (Na$^+$) in the bath solution was replace by equal amount of K$^+$ respectively. In perforated patch clamp, about 500 mg solubilized amphotericin B was added in the pipette solution. Membrane potential changes were analyzed using IGOR software (WaveMetrics, Lake Oswego, OR).

Measurement of ROS production in phagocytic cells

BMDM or PMN (5×10^6) from both $Trpm2^{+/+}$ and $Trpm2^{-/-}$ mice were treated with PMA or LPS. ROS generation in cultured medium was measured using luminol-enhanced chemiluminescence as described [49]. Chemiluminescence was measured in a Wallac 1420 Multilabel Counter (PerkinElmer Life Sciences). Briefly, luminol was added to the co-culture medium to a final concentration of 50 μM, and horseradish peroxidase was added to a final concentration of 40 units/ml. ROS release was determined after cells were stimulated with various stimulus for the indicated times. The relative concentration of ROS in the culture medium was expressed as counts per second.

Fluorometric measurements of intracellular Ca^{2+}

Intracellular Ca^{2+} ([Ca^{2+}]$_i$) was recorded in single cells as described [50]. Briefly, a Zeiss Axiovert 200 (Zeiss, Germany) inverted microscope was illuminated using a Photon Technology International DeltaRam (Monmouth Junction, NJ) dual wavelength monochrometer-based illumination system with a xenon lamp and a Hammamatsu R928 photon counting photomultiplier and optical coupling to the microscope. Cells were loaded with a 2 μM fura-2 AM for 30 min in HBSS at 37^{0}C. Measurement of fura-2 fluorescence at 340 and 380 nm was acquired and offline analyzed using PTI Felix 32 software.

Mortality studies

$Trpm2^{+/+}$ and $Trpm2^{-/-}$ mice (40 mice/group) were injected with LPS (30 mg/kg, i.p.). Percentage of surviving mice was documented every 2 hrs.

Immunoprecipitation and immunoblotting

Activation of PKCα was assessed using antibody that recognizes the phosphorylated forms of PKCα and activation of p47^{phox} was assessed using antibody that recognizes phosphorylated Ser473 after p47 was immunoprecipitated with p47 antibody. Antibodies against non-phosphorylated PKCα and p47 were used to assess protein loading.

Measurement of cytokines and chemokines concentration by enzyme-linked immunosorbent assay (ELISA)

$Trpm2^{+/+}$ and $Trpm2^{-/-}$ mice were sacrificed by i.p. anesthetic at designated time points after LPS injection. Whole lungs were then obtained for measurement of cytokine and chemokine concentration. Lungs were homogenized and centrifuged. Supernatants were

collected for measurement of chemokine concentrations by ELISA using the Bio-Plex Multiplex Cytokine Assay (Bio-Rad).

Lung tissue myeloperoxidase (MPO) activity

Lung tissue MPO activity was measured as described [48]. Briefly, lungs were homogenized and centrifuged and the supernatant was then collected and mixed with assay buffer (0.2 mg/ml o-dianisidine hydrochloride and 0.0005% H_2O_2). Absorbance change was measured at 460 nm for 3 min, and MPO activity was calculated as the change in absorbance over time. PMN sequestration was quantified as MPO activity normalized by the final dry lung weight.

Statistical analysis

Differences in animal survival rate were assessed by log-rank test. Other statistical comparisons were made using two-tailed Student's t test. Experimental values were reported as the means ± S.E.M (standard error of the mean). Significance between groups was determined using the t-test (two tails) and asterisks indicate a significance difference with the number of experiments in parentheses.

Supplementary Material

Refer to Web version on PubMed Central for supplementary material.

ACKNOWLEDGMENTS

REFERENCES

1. Iles KE, Forman HJ. Macrophage signaling and respiratory burst. Immunol Res. 2002; 26:95–105. [PubMed: 12403349]

2. Gwinn MR, Vallyathan V. Respiratory burst: role in signal transduction in alveolar macrophages. J Toxicol Environ Health B Crit Rev. 2006; 9:27–39. [PubMed: 16393868]

3. DeCoursey TE. Voltage-gated proton channels find their dream job managing the respiratory burst in phagocytes. Physiology (Bethesda). 25:27–40. [PubMed: 20134026]

4. DeCoursey TE, Morgan D, Cherny VV. The voltage dependence of NADPH oxidase reveals why phagocytes need proton channels. Nature. 2003; 422:531–4. [PubMed: 12673252]

5. Fontayne A, Dang PM, Gougerot-Pocidalo MA, El-Benna J. Phosphorylation of p47phox sites by PKC alpha, beta II, delta, and zeta: effect on binding to p22phox and on NADPH oxidase activation. Biochemistry. 2002; 41:7743–50. [PubMed: 12056906]

6. Cathcart MK. Regulation of superoxide anion production by NADPH oxidase in monocytes/macrophages: contributions to atherosclerosis. Arterioscler Thromb Vasc Biol. 2004; 24:23–8. [PubMed: 14525794]

7. Nagamine K, Kudoh J, Minoshima S, Kawasaki K, Asakawa S, Ito F, Shimizu N. Molecular cloning of a novel putative Ca2+ channel protein (TRPC7) highly expressed in brain. Genomics. 1998; 54:124–31. [PubMed: 9806837]

8. Sano Y, Inamura K, Miyake A, Mochizuki S, Yokoi H, Matsushime H, Furuichi K. Immunocyte Ca2+ influx system mediated by LTRPC2. Science. 2001; 293:1327–30. [PubMed: 11509734]

9. Owsianik G, Talavera K, Voets T, Nilius B. Permeation and selectivity of TRP channels. Annu Rev Physiol. 2006; 68:685–717. [PubMed: 16460288]

10. Hecquet CM, Ahmmed GU, Vogel SM, Malik AB. Role of TRPM2 channel in mediating H2O2-induced Ca2+ entry and endothelial hyperpermeability. Circ Res. 2008; 102:347–55. [PubMed: 18048770]

11. Lange I, Yamamoto S, Partida-Sanchez S, Mori Y, Fleig A, Penner R. TRPM2 functions as a lysosomal Ca2+-release channel in beta cells. Sci Signal. 2009; 2:ra23. [PubMed: 19454650]

12. Yamamoto S, Shimizu S, Kiyonaka S, Takahashi N, Wajima T, Hara Y, Negoro T, Hiroi T, Kiuchi Y, Okada T, Kaneko S, Lange I, Fleig A, Penner R, Nishi M, Takeshima H, Mori Y. TRPM2-mediated Ca2+influx induces chemokine production in monocytes that aggravates inflammatory neutrophil infiltration. Nat Med. 2008; 14:738–47. [PubMed: 18542050]

13. Guo RF, Ward PA. Role of oxidants in lung injury during sepsis. Antioxid Redox Signal. 2007; 9:1991–2002. [PubMed: 17760509]

14. Chow CW, Abreu M. T. Herrera, Suzuki T, Downey GP. Oxidative stress and acute lung injury. Am J Respir Cell Mol Biol. 2003; 29:427–31. [PubMed: 14500253]

15. Cross AR, Jones OT. The effect of the inhibitor diphenylene iodonium on the superoxide-generating system of neutrophils. Specific labelling of a component polypeptide of the oxidase. Biochem J. 1986; 237:111–6. [PubMed: 3800872]

16. Fonfria E, Marshall IC, Benham CD, Boyfield I, Brown JD, Hill K, Hughes JP, Skaper SD, McNulty S. TRPM2 channel opening in response to oxidative stress is dependent on activation of poly(ADP-ribose) polymerase. Br J Pharmacol. 2004; 143:186–92. [PubMed: 15302683]

17. Suto MJ, Turner WR, Arundel-Suto CM, Werbel LM, Sebolt-Leopold JS. Dihydroisoquinolinones: the design and synthesis of a new series of potent inhibitors of poly(ADP-ribose) polymerase. Anticancer Drug Des. 1991; 6:107–17. [PubMed: 1903948]

18. Ding Y, Yamada S, Wang KY, Shimajiri S, Guo X, Tanimoto A, Murata Y, Kitajima S, Watanabe T, Izumi H, Kohno K, Sasaguri Y. Overexpression of peroxiredoxin 4 protects against high-dose streptozotocin-induced diabetes by suppressing oxidative stress and cytokines in transgenic mice. Antioxid Redox Signal. 13:1477–90. [PubMed: 20446767]

19. Khan SJ, Pham S, Wei Y, Mateo D, St-Pierre M, Fletcher TM, Vazquez-Padron RI. Stress-induced senescence exaggerates postinjury neointimal formation in the old vasculature. Am J Physiol Heart Circ Physiol. 298:H66–74. [PubMed: 19855064]

20. Murphy R, DeCoursey TE. Charge compensation during the phagocyte respiratory burst. Biochim Biophys Acta. 2006; 1757:996–1011. [PubMed: 16483534]

21. Kelkar DA, Chattopadhyay A. The gramicidin ion channel: a model membrane protein. Biochim Biophys Acta. 2007; 1768:2011–25. [PubMed: 17572379]

22. El Chemaly A, Okochi Y, Sasaki M, Arnaudeau S, Okamura Y, Demaurex N. VSOP/Hv1 proton channels sustain calcium entry, neutrophil migration, and superoxide production by limiting cell depolarization and acidification. J Exp Med. 207:129–39. [PubMed: 20026664]

23. Minke B, Cook B. TRP channel proteins and signal transduction. Physiol Rev. 2002; 82:429–72. [PubMed: 11917094]

24. Venkatachalam K, Montell C. TRP channels. Annu Rev Biochem. 2007; 76:387–417. [PubMed: 17579562]

25. Pedersen SF, Owsianik G, Nilius B. TRP channels: an overview. Cell Calcium. 2005; 38:233–52. [PubMed: 16098585]

26. Miller BA. The role of TRP channels in oxidative stress-induced cell death. J Membr Biol. 2006; 209:31–41. [PubMed: 16685599]

27. Hara Y, Wakamori M, Ishii M, Maeno E, Nishida M, Yoshida T, Yamada H, Shimizu S, Mori E, Kudoh J, Shimizu N, Kurose H, Okada Y, Imoto K, Mori Y. LTRPC2 Ca2+-permeable channel activated by changes in redox status confers susceptibility to cell death. Mol Cell. 2002; 9:163–73. [PubMed: 11804595]

28. Wehage E, Eisfeld J, Heiner I, Jungling E, Zitt C, Luckhoff A. Activation of the cation channel long transient receptor potential channel 2 (LTRPC2) by hydrogen peroxide. A splice variant

reveals a mode of activation independent of ADP-ribose. J Biol Chem. 2002; 277:23150–6. [PubMed: 11960981]

29. Randriamampita C, Trautmann A. Biphasic increase in intracellular calcium induced by platelet-activating factor in macrophages. FEBS Lett. 1989; 249:199–206. [PubMed: 2544447]

30. Swain SD, Bunger PL, Sipes KM, Nelson LK, Jutila KL, Boylan SM, Quinn MT. Platelet-activating factor induces a concentration-dependent spectrum of functional responses in bovine neutrophils. J Leukoc Biol. 1998; 64:817–27. [PubMed: 9850166]

31. Vennekens R, Olausson J, Meissner M, Bloch W, Mathar I, Philipp SE, Schmitz F, Weissgerber P, Nilius B, Flockerzi V, Freichel M. Increased IgE-dependent mast cell activation and anaphylactic responses in mice lacking the calcium-activated nonselective cation channel TRPM4. Nat Immunol. 2007; 8:312–20. [PubMed: 17293867]

32. Nilius B, Prenen J, Droogmans G, Voets T, Vennekens R, Freichel M, Wissenbach U, Flockerzi V. Voltage dependence of the Ca2+-activated cation channel TRPM4. J Biol Chem. 2003; 278:30813–20. [PubMed: 12799367]

33. Colquhoun D, Neher E, Reuter H, Stevens CF. Inward current channels activated by intracellular Ca in cultured cardiac cells. Nature. 1981; 294:752–4. [PubMed: 6275271]

34. Prawitt D, Monteilh-Zoller MK, Brixel L, Spangenberg C, Zabel B, Fleig A, Penner R. TRPM5 is a transient Ca2+-activated cation channel responding to rapid changes in [Ca2+]i. Proc Natl Acad Sci U S A. 2003; 100:15166–71. [PubMed: 14634208]

35. Launay P, Fleig A, Perraud AL, Scharenberg AM, Penner R, Kinet JP. TRPM4 is a Ca2+-activated nonselective cation channel mediating cell membrane depolarization. Cell. 2002; 109:397–407. [PubMed: 12015988]

36. Sumoza-Toledo A, Lange I, Cortado H, Bhagat H, Mori Y, Fleig A, Penner R, Partida-Sanchez S. Dendritic cell maturation and chemotaxis is regulated by TRPM2-mediated lysosomal Ca2+ release. Faseb J. 2011; 25:3529–42. [PubMed: 21753080]

37. Sumoza-Toledo A, Penner R. TRPM2: A Multifunctional Ion Channel for Calcium Signaling. J Physiol. 2011; 589:1515–1525. [PubMed: 21135052]

38. Schrenzel J, Serrander L, Banfi B, Nusse O, Fouyouzi R, Lew DP, Demaurex N, Krause KH. Electron currents generated by the human phagocyte NADPH oxidase. Nature. 1998; 392:734–7. [PubMed: 9565037]

39. Klebanoff SJ. Oxygen metabolism and the toxic properties of phagocytes. Ann Intern Med. 1980; 93:480–9. [PubMed: 6254418]

40. Bankers-Fulbright JL, Gleich GJ, Kephart GM, Kita H, O'Grady SM. Regulation of eosinophil membrane depolarization during NADPH oxidase activation. J Cell Sci. 2003; 116:3221–6. [PubMed: 12829741]

41. Petheo GL, Demaurex N. Voltage- and NADPH-dependence of electron currents generated by the phagocytic NADPH oxidase. Biochem J. 2005; 388:485–91. [PubMed: 15689187]

42. Demaurex N, Elchemaly A. Physiological roles of voltage-gated proton channels in leukocytes. J Physiol.

43. Buckley JF, Singer M, Clapp LH. Role of KATP channels in sepsis. Cardiovasc Res. 2006; 72:220–30. [PubMed: 16963005]

44. Zorn-Pauly K, Pelzmann B, Lang P, Machler H, Schmidt H, Ebelt H, Werdan K, Koidl B, Muller-Werdan U. Endotoxin impairs the human pacemaker current If. Shock. 2007; 28:655–661. [PubMed: 18092381]

45. Umans JG, Salvi D, Murray PT, Wylam ME. Selectivity of endotoxin-induced defect in endothelial calcium mobilization. Kidney Int. 1998; 54:1063–9. [PubMed: 9767522]

46. Zhang X, Goncalves R, Mosser DM. The isolation and characterization of murine macrophages. Curr Protoc Immunol. 2008:1. Chapter 14, Unit 14. [PubMed: 19016445]

47. Xu J, Gao XP, Ramchandran R, Zhao YY, Vogel SM, Malik AB. Nonmuscle myosin light-chain kinase mediates neutrophil transmigration in sepsis-induced lung inflammation by activating beta2 integrins. Nat Immunol. 2008; 9:880–6. [PubMed: 18587400]

48. Garrean S, Gao XP, Brovkovych V, Shimizu J, Zhao YY, Vogel SM, Malik AB. Caveolin-1 regulates NF-kappaB activation and lung inflammatory response to sepsis induced by lipopolysaccharide. J Immunol. 2006; 177:4853–60. [PubMed: 16982927]

49. Gao XP, Zhu X, Fu J, Liu Q, Frey RS, Malik AB. Blockade of class IA phosphoinositide 3-kinase in neutrophils prevents NADPH oxidase activation- and adhesion-dependent inflammation. J Biol Chem. 2007; 282:6116–25. [PubMed: 17197441]

50. Di A, Krupa B, Nelson DJ. Calcium-G protein interactions in the regulation of macrophage secretion. J Biol Chem. 2001; 276:37124–32. [PubMed: 11479305]
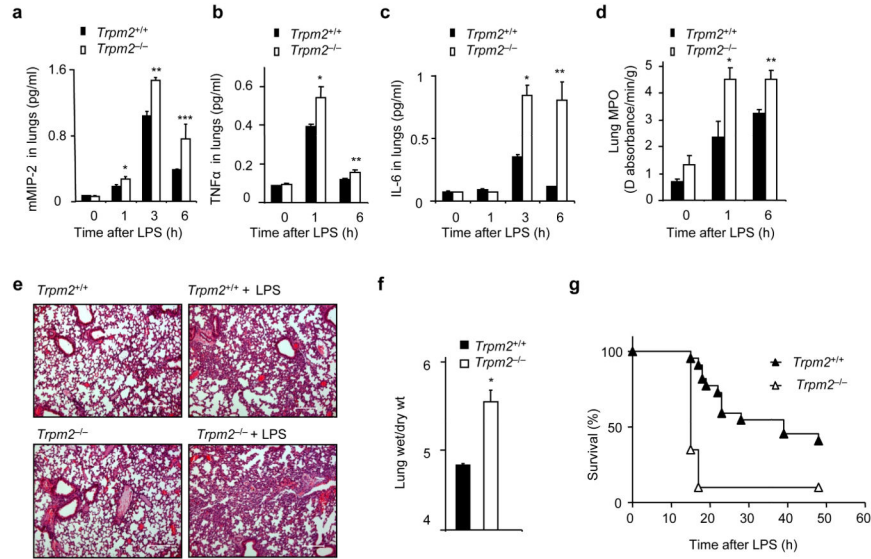
Figure 1. TRPM2 deletion augmented endotoxin-induced lung inflammation and injury
(**a-c**). Augmented LPS-induced production of MIP-2 (**a**), TNFα (**b**), and IL-6 (**c**) in mouse lung after LPS (10 mg/kg, i.p.) challenge in *Trpm2*$^{-/-}$ mice. (**a**). *p = 0.036 (n = 6), **p = 0.0003 (n = 6), ***p = 0.0008 (n = 6), compared to *Trpm2*$^{+/+}$ *group;* (**b**). *p = 0.036 (n = 6), **p = 0.037 (n = 6), compared to *Trpm2*$^{+/+}$ *group;* (**c**). *p = 0.018 (n = 6), **p = 0.005 (n = 6), compared to *Trpm2*$^{+/+}$ *group*. (**d**) Lung PMN sequestration as measured by tissue MPO activity. Mice were challenged with LPS (10 mg/kg, i.p.) for the times indicated. *p = 0.055 (n = 3), **p = 0.022 (n = 5), compared to *Trpm2*$^{+/+}$ *group*. (**e**) H&E (hematoxylin and eosin) staining of lung tissue sections isolated from *Trpm2*$^{+/+}$ and *Trpm2*$^{-/-}$ mice challenged with LPS (20 mg/kg, i.p.) for 20 hr. Note the enhanced inflammatory cell infiltration in *Trpm2*$^{-/-}$ lung after LPS challenge. Scale bar, 200 μm. (**f**) Pulmonary edema formation in *Trpm2*$^{+/+}$ and *Trpm2*$^{-/-}$ lungs after LPS challenge (20 mg/kg, i.p.). Edema was measured by increase in wet weight of lungs. *p = 0.006 (n = 3). (**g**). TRPM2 expression protects mice from LPS-induced death. Both *Trpm2*$^{+/+}$ and *Trpm2*$^{-/-}$ mouse survival rates were calculated after LPS i.p. injection (30 mg/kg). Differences in mortality were determined by log-rank test (p = 0.0007, n = 40 each).
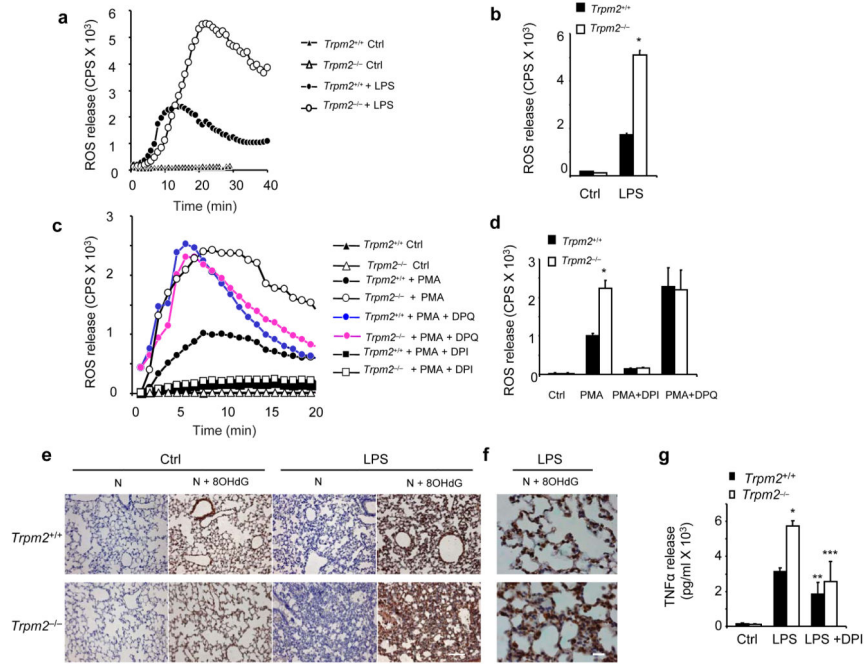
Figure 2. TRPM2 deletion enhanced ROS generation and oxidative lung inflammatory injury
(**a-d**). TRPM2 ablation enhances ROS release from *Trpm2*$^{-/-}$ PMN stimulated with LPS (1 μg/ml, **a-b**) and *Trpm2*$^{-/-}$ BMDM stimulated with PMA (1 μM, **c-d**) compared with cells from *Trpm2*$^{+/+}$ mice. *cps*=counts per second of light emitted. DPI prevented the increased ROS production in both *Trpm2*$^{+/+}$ and *Trpm2*$^{-/-}$ BMDM. Note that pretreatment with DPQ (100 μM, 30 min at 37^{0}C) augmented ROS release in *Trpm2*$^{+/+}$ cells but not in *Trpm2*$^{-/-}$ cells. *p = 0.00007 (n= 3) in **b** and *p = 0.007 (n = 6) in **d**. **e-f.** Immunohistochemical detection of 8-OHdG in lung sections from *Trpm2*$^{+/+}$ and *Trpm2*$^{-/-}$ mice challenged with LPS (20 mg/kg) for 20 hr with lower magnification in **e** (scale bar, 100 μm) and higher magnification in **f** (scale bar, 20 μm). Nuclei were stained with hematoxylin (blue color, labeled as "N" in the figure). 8-OHdG (brown color) expression was weak in untreated mouse lung (control) and was increased after LPS stimulation in both *Trpm2*$^{-/-}$ and *Trpm2*$^{+/+}$ group. (**g**). Augmented LPS-induced production of TNFα from mouse BMDM was NADPH oxidase sensitive. *p = 0.00003 (n = 7) compared to *Trpm2*$^{+/+}$ + LPS group; **p = 0.046 (n = 3) compared to *Trpm2*$^{+/+}$ + LPS group. ***p = 0.013 (n = 3) compared to *Trpm2*$^{-/-}$ + LPS group.
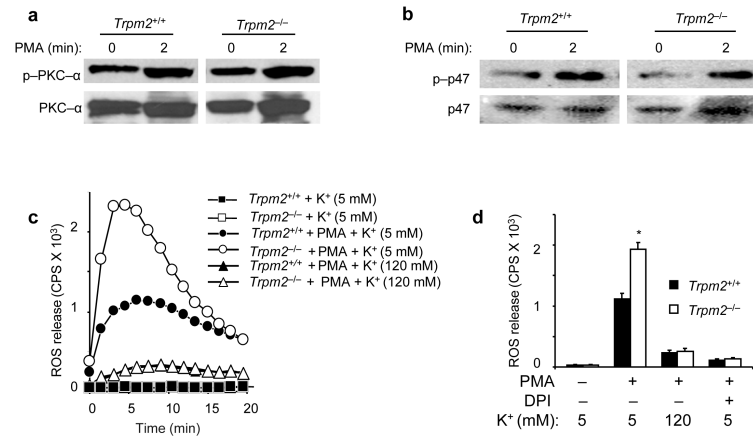
Figure 3. TRPM2 had no effect on phosphorylation of PKCα and p47^{phox} and high extracellular potassium inhibited ROS production in both *Trpm2*$^{−/−}$ and *Trpm2*$^{+/+}$ macrophages

(**a**) Phosphorylation of PKCα of BMDM from *Trpm2*$^{+/+}$ or *Trpm2*$^{−/−}$ mice. BMDM were stimulated with PMA (1 μM) for 2 min. Equal protein loading was verified by membrane probing with anti-PKCα antibodies. TRPM2 expression did not affect phosphorylation of PKCα in BMDM stimulated with PMA. (**b**) Phosphorylation of p47^{phox} of BMDM pretreated with PMA (1 μM) for 2 min. Phosphorylation was evaluated by immunoprecipitation of p47^{phox} and immunoblotting with antibodies against phosphoserine and p47^{phox}. Note that TRPM2 expression did not regulate the phosphorylation of p47^{phox} in BMDM stimulated with PMA. (**c**) Representative curves of ROS release in BMDM from both *Trpm2*$^{+/+}$ BMDM and *Trpm2*$^{−/−}$ BMDM under different extracellular potassium concentration ([K$^+$]$_{out}$). These curves showed that pre-depolarization of BMDM by incubating cells with high K$^+$ (120 mM) abrogated the differences in ROS production between *Trpm2*$^{+/}$ and *Trpm2*$^{−/−}$ BMDM stimulated with PMA (1 μM). *cps*, counts per second of light emitted. (**d**) Summary of data obtained in (**C**). The figure shows ROS generation decreased with high extracellular concentration of K$^+$ which depolarized the cell plasma membrane. *$p = 0.015$ (n = 5) compared with *Trpm2*$^{+/+}$ group.
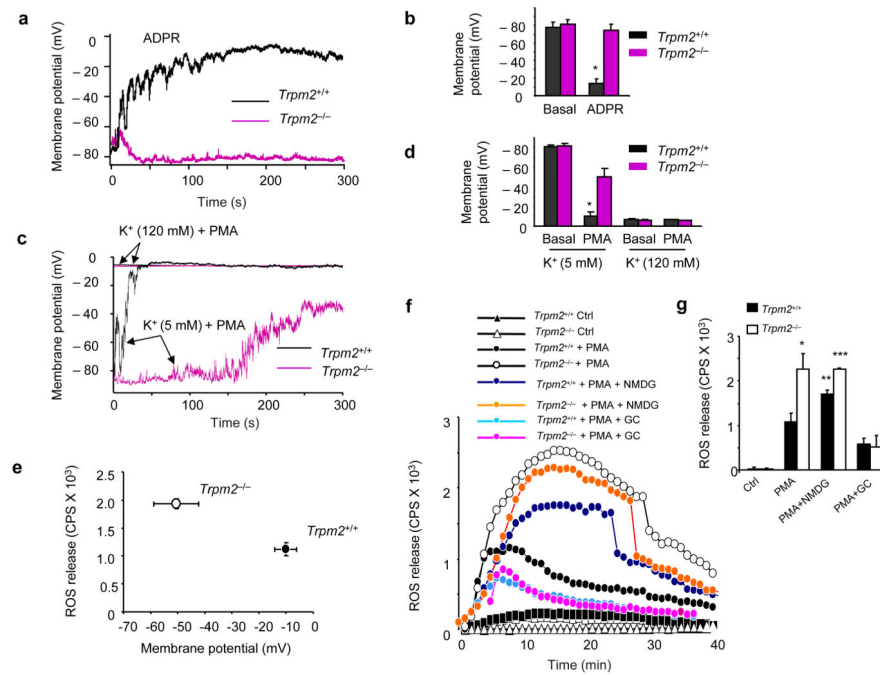
Figure 4. TRPM2 inhibited ROS production in macrophages through plasma membrane depolarization

(**a-b**) The TRPM2 activator ADPR failed to depolarize the plasma membrane in the absence of TRPM2 expression in BMDM. Representative curves showing plasma membrane potential changes are shown in (**a**) and the summary is shown in (**b**). *p = 0.0005 (n = 6) compared with $Trpm2^{-/-}$ + ADPR group. (**c-d**) PMA (1 μM) failed to fully depolarize the plasma membrane in the absence of TRPM2 expression in BMDM. Representative curves showing changes in plasma membrane potential are shown in (**c**) and summary is shown in (**d**). *p = 0.0005 (n = 15) compared with $Trpm2^{+/+}$ group. (**e**) Correlation of membrane potential with ROS production in BMDM. Figure is reconstituted partly from data shown in Figure **3d** and Figure **4d**. Cells were stimulated with PMA (1 μM) in the presence of 5 mM K$^+$ in the extracellular solution. (**f-g**) ROS release in both $Trpm2^{+/+}$ and $Trpm2^{-/-}$ BMDM stimulated with PMA (1 μM) under physiological and controlled membrane potential. These curves show that pre-depolarization of BMDM by incubating cells with gramicidin (GC, 40μg/ml) not only inhibited ROS release from both $Trpm2^{+/+}$ BMDM and $Trpm2^{-/-}$ BMDM, but also abrogated the differences in ROS production between $Trpm2^{+/+}$ and $Trpm2^{-/-}$ BMDM. Note that replacement of Na$^+$ with NMDG augmented ROS release in $Trpm2^{+/+}$ BMDM while it had little effect of ROS release from $Trpm2^{-/-}$ BMDM. *p = 0.0003 (n = 6) and **p = 0.0006 (n = 4) compared to $Trpm2^{+/+}$ + PMA group.
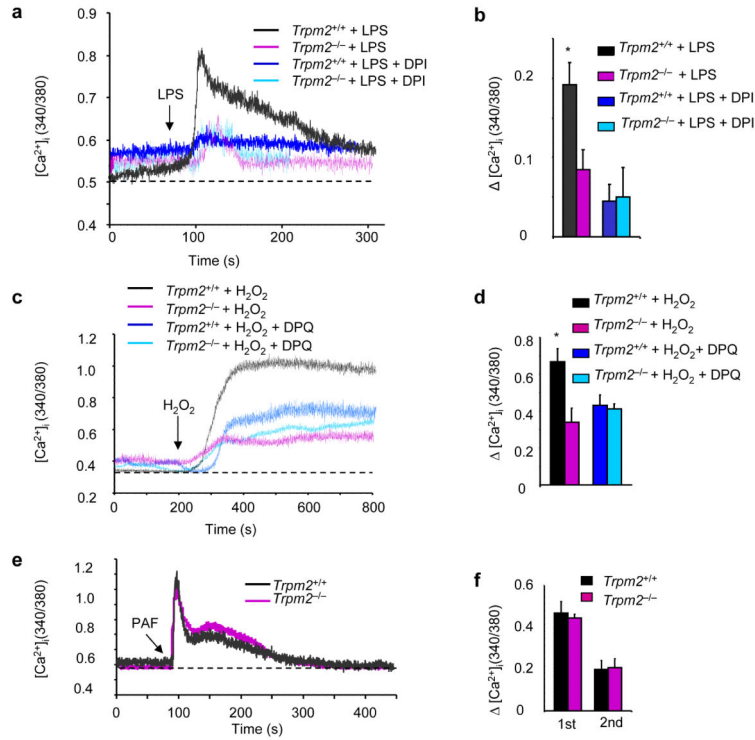
Figure 5. LPS -induced Ca^{2+} entry in macrophages was dependent on TRPM2 expression
(**a-b**). TRPM2 ablation reduced LPS-induced ROS-dependent [Ca^{2+}]$_i$ increase in mouse macrophages. Typical recordings are displayed in **a** and the average results are shown in **b**. LPS (1μg/ml) induced a rapid [Ca^{2+}]$_i$ increase in *Trpm2*$^{+/+}$ BMDM but [Ca^{2+}]$_i$ increase induced by LPS was significantly reduced in *Trpm2*$^{-/-}$ BMDM. The [Ca^{2+}]$_i$ increase in *Trpm2*$^{+/+}$ cells pretreated with DPI (1μM) was reduced to the same level as in *Trpm2*$^{-/-}$ cells treated with same amount of DPI. Data are mean of changes in ratiometric values from basal to steady-state [Ca^{2+}]$_i$. *p = 0.001 (n = 5) compared with *Trpm2*$^{-/-}$ group. (**c-d**). DPQ-pretreatment reduced H2O2-induced [Ca^{2+}]$_i$ increase in mouse macrophages. Typical recordings are displayed in **c** and the average results are shown in **d**. *p = 0.008 (n = 7) compared with *Trpm2*$^{-/-}$ group. (**e-f**). TRPM2-ablation did not altered PAF-induced [Ca^{2+}]$_i$ increase in mouse macrophages. Typical recordings are displayed in **c** and average results are shown in **d**. PAF (0.1μM) induced a rapid [Ca^{2+}]$_i$ increase followed by a slow [Ca^{2+}]$_i$ increase in both *Trpm2*$^{+/+}$ BMDM and *Trpm2*$^{-/-}$ BMDM. The amplitudes of the two peaks were calculated by measuring changes in ratiometric values from basal to steady-state [Ca^{2+}]$_i$ and summarized in **d**. Data are mean of changes in ratiometric values from basal to steady-state [Ca^{2+}]$_i$ (n = 4-5).